Published in "ECS Electrochemistry Letters 1(4): F25-F28, 2012"
which should be cited to refer to this work.

Electrochemical Characterization of Porous Diaphragms in Development for Gas Separation

J. Stojadinović,[a,z] D. Wiedenmann,[a,b] M. Gorbar,[a] F. La Mantia,[c] L. Suarez,[a] V. Zakaznova-Herzog,[a] U. F. Vogt,[a] B. Grobéty,[b] and A. Züttel[a]

[a]*EMPA, Materials Science and Technology, Hydrogen & Energy, Dübendorf, Switzerland*
[b]*University of Fribourg, Department Geosciences and FRIMAT, Fribourg, Switzerland*
[c]*University of Bochum, Department Chemistry and Biochemistry, Germany*

The alkaline electrolyzer industry is facing the imminent necessity of replacing the asbestos diaphragms with a separator made of a new environmentally friendly material. The influence of a diaphragm's material and porosity on the ionic conductivity was studied for asbestos, zirconium dioxide, wollastonite and olivine diaphragms. Developed electrochemical impedance spectroscopy (EIS) set-up with four-electrode cell offers the possibility for an accurate measurement of diaphragms' ionic conductivity and enables its correlation to the materials porosity and tortuosity. The ion conductivity of investigated diaphragms approaches zero value for total porosities below 20% and increases when increasing porosities in agreement with Archie's law.

The efficiency of high pressure alkaline electrolysis is highly influenced by the properties of the diaphragm which separates the hydrogen and oxygen gases, mounted between the anode and cathode.[1] Diaphragms should provide high ionic conductivity, but exhibit a barrier for the interpenetration of hydrogen and oxygen gases. Furthermore, the diaphragm must withstand extreme conditions, up to 30 wt% KOH and 120°C in highly oxidative and reductive environments on the oxygen and hydrogen electrodes, respectively.

According to the European Commission regulations[2] asbestos diaphragms, which are still a part of high pressure zero gap alkaline electrolyzers, can only be used in existing electrolyzers until the end of their service life, or until suitable substitutes become available. New electrolyzers are only allowed without asbestos diaphragms. Different porous composite materials based on polymers (e.g. polysulfone) and ceramics (e.g. ZrO_2 particles) are being developed to replace asbestos diaphragms.[1,3,4,5]

Energy losses in electrolyzers are caused by ohmic resistance in the electron and ion conducting parts (current collectors, electrode bulk, electrolyte and diaphragm) and by anodic and cathodic overpotentials.[6] Therefore, one direction for the improvement of alkaline electrolyzers efficiency is the reduction of energy losses through the increase of the ionic conductivity,[7] while maintaining the requirement for high gas purity.

The internal cell resistance, R_c, can be expressed as:[7–9]

$$R_c = R_{an} + R_{cat} + R_D \quad [1]$$

where R_{an}, R_{cat} and R_D are anolyte, catholyte and diaphragm resistances, respectively.The diaphragm resistance, R_D [Ω], was correlated to porosity, ε, by Vermeiren at al.:[4]

$$R_D = \rho_{el} L \frac{\tau^2}{\varepsilon A \omega} \quad [2]$$

where ρ_{el} is the ionic resistivity of the electrolyte, L is the diaphragm thickness, τ is the tortuosity (defined as the ratio of actual pore lengths and diaphragm thickness), ε is the porosity, A the cross sectional surface of a diaphragm and ω is the wettability factor.

Van der Stegen et al.[10] have demonstrated that the major parameters which determine the ionic conductivity of diaphragms (asbestos and non-asbestos) are the diaphragm thickness, pore size distribution and the number of interconnects among pores inside the diaphragm. The effects of porosity and pore distribution on ionic conductivity remained topics of interest, due to lack of understanding.[10] Our study provides the electrochemical methodology which together with an extended pore structure model, including the geometric parameters for constrictivity and tortuosity,[11] enables the calculation of the ion conductivity of porous and electrically isolating materials.

[z]E-mail: jelena.stojadinovic@rub.de

Experimental

Materials and solutions.— Ceramic diaphragms were prepared by mechanical uniaxial pressing of granular 3 mol.% Y_2O_3 stabilized ZrO_2 powder under the pressure of 36 MPa. Different porosities were obtained (42, 45 and 53%) by varying the content of carbon pore former (0, 20 and 40 vol.%) and sintering the samples at 1200°C (in order to eliminate carbon). The same procedure was used for the preparation of ceramic mineral diaphragms composed of olivine [$(Mg,Fe)_2SiO_4$, provided by North Cape Minerals, Krefeld, Germany] and wollastonite ($CaSiO_3$, provided by Mial, Feldmeilen, Switzerland), with porosities ranging from 27% to 44%, and from 45% to 80%, respectively. In addition, asbestos [$Mg_3Si_2O_5(OH)_4$] samples (porosity 65%) supplied by IHT Monthey, Switzerland, were investigated.

The porosity of olivine, wollastonite and asbestos samples was determined using synchrotron X-ray absorption tomography.[11,12] The porosity of ZrO_2 samples was obtained using the water absorption method, due to the fact that the detailed tomographic features of these samples were not important for practical application.

All diaphragms had a diameter of 20 mm and a thickness of 2.5 mm. An asbestos sample was fixed between two perforated PTFE disks prior to installation in the electrochemical cell. The diaphragm surface area exposed to the electrolyte in a half-cell was 2 cm^2, with O-rings mounted on both sides covering the edges of the diaphragm. Prior to experiments the samples were immersed in 25 wt% KOH solution for 15 min.

Nickel electrodes (99.95% purity) served as cathode and anode in the electrochemical set-up. Prior to experiments the Ni electrodes were polished with SiC grit paper 1000, rinsed with distilled water and dried with compressed air.

The electrolyte used for all experiments was 5.5 M KOH (25 wt%). All tests were performed at room temperature (21–23°C).

Electrochemical impedance spectroscopy (EIS).— A four-electrode, two-compartment electrochemical cell (Fig. 1) placed in a Faraday's cage and connected to Zahner IM6eX potentiostat, operating with Thales 4.05 USB software, was used for EIS measurements. Two Ni disk electrodes served as anode (working electrode, WE, oxygen evolution) and cathode (counter electrode, CE, hydrogen evolution). Diaphragms (D) were mounted between two Hg/HgO reference electrodes filled with 1 M KOH (0.112 V vs. standard hydrogen electrode, SHE, at 25°C), acting as a reference (RE) and sense electrode (SE) (Fig. 1). Both SE and RE were modified by a "by-pass" using Pt wire and a 0,1 μF capacitor. Potentials in this paper always refer to the standard hydrogen electrode.

Frequencies were swept from 100 KHz to 100 mHz in the potentiostatic mode. Potentiostatic mode was chosen over the galvanostatic mode in order to avoid the non-linear response of the system, often encountered at lower frequencies. The current flowing between the

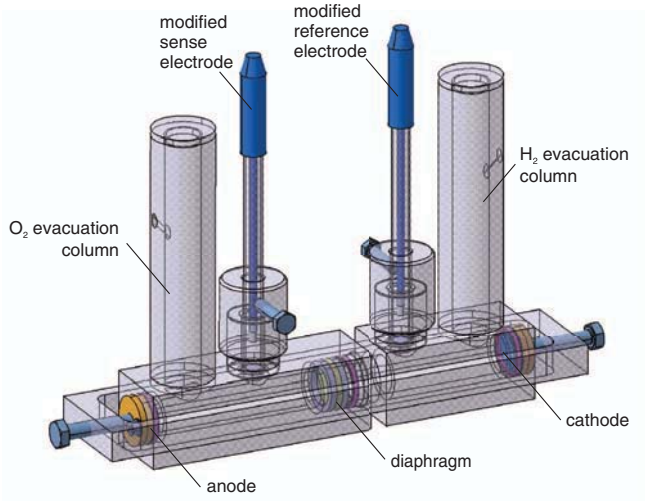

Figure 1. Four-electrode two-compartment electrochemical cell.

working and the counter electrode varied with the type of diaphragm installed in the cell, while the imposed potential between the sense and reference electrodes was kept constant at the value of 0.75 V. The AC amplitude was set to 10 mV. The applied potential enabled experiments to be performed in the electrolysis regime, while moderate amounts of gases are generated and the cell temperature increase was negligible. Performing experiments in the electrolysis regime was chosen in order to attempt to approach the real industrial conditions.

When a diaphragm was mounted in the cell, the distance between the anode and cathode was 156.5 mm, while the distance between the sense and the reference electrode was 66.5 mm (Fig. 2a and 2c).

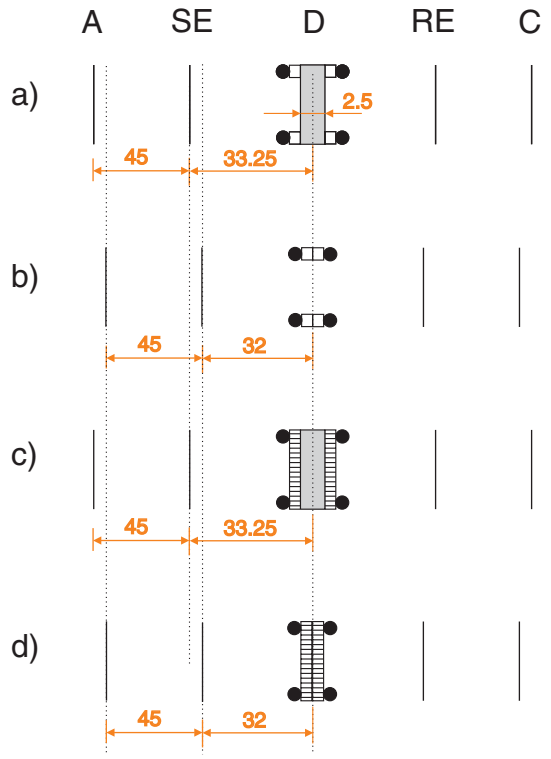

Figure 2. Distances between A-SE and SE-D: a) with installed brittle diaphragm, b) without a diaphragm, c) with mounted flexible asbestos diaphragm and perforated PTFE disks and d) with perforated PTFE disks only. Comment: Dimensions given in mm. The cell geometry is symmetrical taking into account the diaphragm position as the referent plane.

Without a mounted diaphragm, the electrodes were brought closer to compensate for the diaphragm thickness,[13] thus the distances between A-C and SE-RE were 154 mm and 64 mm, respectively (Fig. 2b and 2d).

Wollastonite, olivine and ZrO_2 diaphragms were mounted in the cell with two rubber O-rings and PTFE (Polytetrafluoroethylene) rings on both sides, as depicted in Fig. 2a. For asbestos diaphragms perforated PTFE disks were placed on both sides to prevent swelling of the cloth-like asbestos diaphragm (Fig. 2c).

Each experiment was performed three times to check for reproducibility.

The four-electrode electrochemical cell (Fig. 1) was also used for the measurements of 5.5 M KOH conductivity, without the diaphragm mounted in the cell (Fig. 2b).

Results

Electrolyte conductivity measurements.— To calculate the cell constant, K (Eq. 3), the resistance, R_{st}, of two standard electrolytes, 0.1 M KCl and 1 M KCl, of known conductivity, k_{st}, was measured using the four-electrode cell (Fig. 1).

$$K = k_{st} R_{st} \quad [3]$$

Electrolyte resistance, R_{el}, (Table I) was measured as explained in section 2.2 for the set up presented in Fig. 2b. The ionic conductivity of the 5.5 M KOH electrolyte was calculated using:

$$k = \frac{K}{R_{el}} \quad [4]$$

Diaphragm resistance determination by EIS.— The performed EIS measurements were used for determination of the cell impedance, Z:

$$Z = Z_{\mathrm{Re}} + j Z_{\mathrm{Im}} \quad [5]$$

where Z is the complex impedance, with Z_{Re} and Z_{Im} the real and imaginary parts of the complex impedance, respectively. The imaginary part of the complex impedance (Fig. 3) for all performed measurements lie in the milliohm range (from approx. 0.5 to 3 mΩ) and can be neglected compared to the real part of impedance lying in the ohm range (from approx. 4 to 7 Ω). Therefore, the measured Z_{Re}, represents the cell resistance, R_c, (Table II).

Knowing the values of R_c and R_{el} the diaphragm resistance, R_D, can then be calculated:

$$R_D = R_c - R_{el} \quad [6]$$

The EIS measurements performed with perforated PTFE disks, both with and without a diaphragm (Fig. 2c and 2d), gave the values of the cell resistance with mounted asbestos and perforated PTFE disks, $R_{c,m}$, and the cell resistance with only perforated PTFE disks, $R_{el,m}$ (5.07 ± 0.06 Ω). This allowed determination of the asbestos diaphragm resistance:

$$R_D = R_{c,m} - R_{el,m} \quad [7]$$

Table I. Determination of the cell constant, K, and 5.5 M KOH conductivity, k, using standard 0.1 M KCl and 1M KCl.

Electrolyte	R_{st}, Ω	k_{st}, mS/cm	K, cm^{-1}
0.1 M KCl	214.95	12.85	2.76
0.1 M KCl	212.38	12.85	2.73
1 M KCl	24.97	111.30	2.78
1 M KCl	24.99	111.30	2.78
	R_{el}, Ω	k, mS/cm	
5.5 M KOH	4.29 ± 0.00	644.57 ± 0.71	

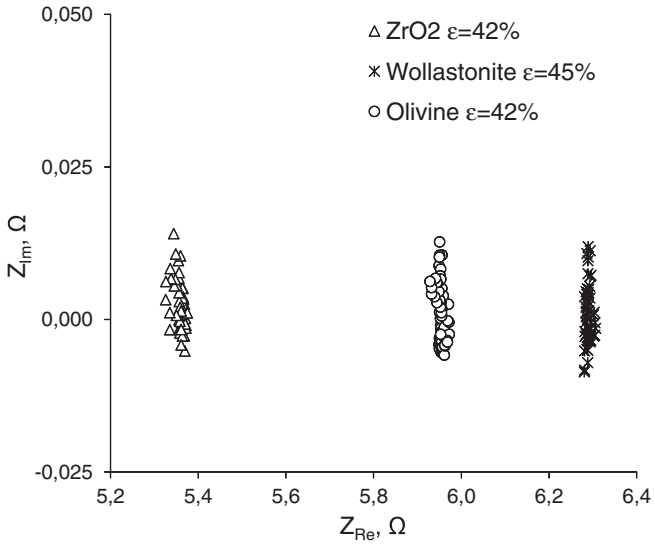

Figure 3. EIS spectra of three different isolating dipahragms. The pore space is filled with electrolyte.

Discussion

The tortuosity, τ, model can be developed based on Eq. 8 and Eq. 10, where k is the electrolyte conductivity, l is the average pore length in a diaphragm, A_p is the cross sectional diaphragm's surface containing only pores, A is the apparent cross sectional diaphragm's surface, ε is the total porosity of diaphragm material and L is the thickness of the diaphragm.

$$R_D = \frac{l}{kA_p} \quad [8]$$

$$A_p = \varepsilon A \quad [9]$$

$$l = L\tau \quad [10]$$

$$R_D = \frac{L\tau}{k\varepsilon A} \quad [11]$$

$$\tau = \frac{R_D k \varepsilon A}{L} \quad [12]$$

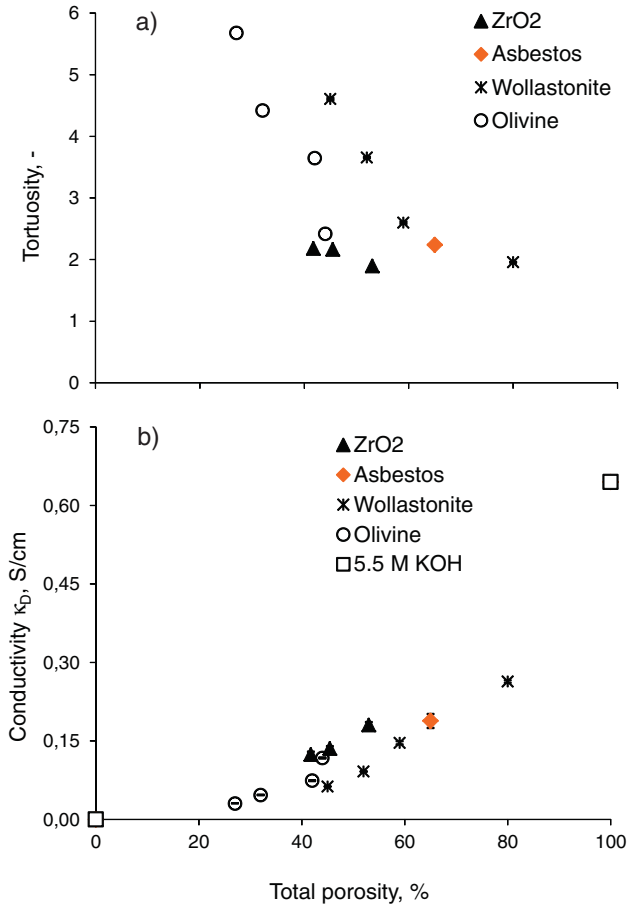

Figure 4. a) Tortuosity of different porous diaphragms versus total porosity and b) conductivity determined by EIS for investigated porous diaphragms versus total porosity.

Tortuosity of the investigated diaphragms (Fig. 4a) calculated using the model (Eq. 12) represents the electric tortuosity.[11] In the case of a system with non-constricted pore paths[14] the geometric tortuosity, τ_{geo}, is equal to the electric tortuosity. Nevertheless, the porous diaphragms in our study are a complex porous system. To determine the geometric tortuosity of the complex porous systems it is necessary to define the constrictivity of the porous material, which is explained elsewhere.[11] If in Eq. 11 the geometric tortuosity is used, instead of

Table II. Influence of diaphragm material and total porosity, ε, on measured cell resistance, R_c, current, I, calculated diaphragm resistance, R_D and electric tortuosity, τ.

Diaphragm material	ε,%	R_c, Ω	I, mA	R_D, Ω	τ, -
ZrO2	42	5.30 ± 0.04	140.44 ± 0.72	1.01 ± 0.05	2.18
	45	5.21 ± 0.03	142.41 ± 0.22	0.92 ± 0.03	2.16
	53	4.98 ± 0.02	152.55 ± 0.47	0.69 ± 0.02	1.90
Asbestos[a]	65	5.74 ± 0.05	128.18 ± 0.74	0.67 ± 0.05	2.24
Wollastonite	45	6.27 ± 0.01	119.67 ± 0.32	1.98 ± 0.01	4.61
	52	5.65 ± 0.01	131.40 ± 0.30	1.36 ± 0.01	3.66
	59	5.14 ± 0.02	145.75 ± 0.59	0.85 ± 0.02	2.60
	80	4.76 ± 0.00	157.99 ± 0.13	0.47 ± 0.00	1.96
Olivine	27	8.36 ± 0.02	89.30 ± 0.23	4.07 ± 0.02	5.68
	32	6.96 ± 0.02	107.39 ± 0.37	2.68 ± 0.02	4.42
	42	5.97 ± 0.02	126.06 ± 0.29	1.68 ± 0.02	3.65
	44	5.35 ± 0.01	138.95 ± 0.32	1.06 ± 0.01	2.42

[a] Asbestos diaphragm cell resistance in this table corresponds to $R_{c,m}$ i.e. resistance with mounted asbestos and perforated PTFE disks (Fig. 2).

the electric one, an overestimation of the apparent conductivity of the diaphragms is obtained, for which the geometric tortuosity is always smaller than the electric one.

The conductivity, k_D, (Fig. 4a), corresponding to the conductivity of the electrolyte in the pores, was calculated for all diaphragms using:

$$k_D = k\frac{\varepsilon}{\tau} \quad [13]$$

According to Archie[15] and McLachlan[16] the conductivity of samples made of the same material, though with different porosities, can be characterized by the exponential function (Eq. 14). The exponent, m, depends on material properties, such as the charge on the pore walls, and pore network. All the mass transport relevant microstructural parameters other than porosity (i.e. tortuosity, constrictivity) are contained in the exponent m:[11]

$$\frac{k_D}{k} = \varepsilon^m \quad [14]$$

The charge on the pore walls is related to the potential of the outer Helmholtz plane.[13] For uncharged pores the conductivity in the pores is equal to the bulk conductivity, because the distribution of ions in the vicinity of the pore walls is identical to their distribution in the bulk electrolyte. The total porosity effect comprises the interplay of the pore charge and pore network[13] for a given material.

Different conductivity observed for similar porosities in Fig. 4b can be attributed to the difference in the microstructural parameters, such as the interconnectivity of the pores[10] or pore geometry. A systematic difference between olivine and wollastonite samples is observed with an increase of porosity (Fig. 4a, Fig. 4b), while zirconia samples follow the trends for olivine. This can be explained with the granular structure (non-fibrous) of olivine and zirconia, in contrast to the acicular habit (fibrous structure) of wollastonite. Rounded olivine and zirconia grains and acicular wollastonite grains differ in the way that the former form isometric, while the later form elongated pores.[11]

Conductivity curves for each material (Fig. 4b) follow Eq. 14, representing a structure dependent relation including Archie's factor, m.[11] They are flat from 0% to approx. 20% porosity and increase to 100% porosity, reaching the conductivity of the electrolyte itself.

The presented method for determination of the diaphragms conductivity and electric tortuosity together with the microstructure quantification methods, giving information on constrictivity and geometric tortuosity directly from tomographs,[11] allow for the fundamental study of a transport in porous media with a wide application in alkaline electrolysis, fuel cells and batteries.

Conclusions

Electrochemical impedance spectroscopy undertaken using a developed system with two-compartment four-electrode cell offers the possibility of an accurate measurement of the impedance of insulating porous diaphragms mounted between the compartments.

The imaginary part of impedance is negligible compared to the real part for the whole frequency range indicating that the impedance has purely resistive character for all investigated diaphragms.

Calculated electric tortuosities, τ, contain all mass transport relevant microstructural parameters other than porosity. To determine the geometric tortuosity (τ_{geo}) of a complex porous system, the constrictivity of the porous material needs to be assessed.

The ionic conductivity of the investigated diaphragms approaches zero for total porosities below approx. 20%.

For olivine (non-fibrous structure) and wollastonite (fibrous structure) diaphragms, whose porosities were assessed using the same method, it is clearly shown that the material has an effect on the ion conductivity. The non-fibrous zirconia diaphragms follow the olivine trend.

Acknowledgment

This work was supported by the Swiss Federal Commission for Technology and Innovation CTI (Ref. 8574.2 PFIW-IW), Bundesamt für Energie BFE (Ref. SI/500576) and SwissElectric Research.

List of Symbols

A	Diaphragm's apparent cross sectional surface, cm^2
A_p	Cross sectional diaphragm's surface containing only pores, cm^2
I	Current during EIS measurements, mA
K	Cell constant, cm^{-1}
l	Average pore length in a diaphragm, mm
L	Diaphragm thickness, mm
m	exponent comprising material properties (ex. pore network), -
R_{an}	Anolyte resistance, Ω
R_c	Internal cell resistance, Ω
R_{cat}	Catholyte resistance, Ω
$R_{c,m}$	Cell resistance with mounted asbestos and perforated PTFE disks, Ω
R_D	Diaphragm resistance, Ω
R_{el}	Electrolyte resistance, Ω
$R_{el,m}$	Cell resistance with perforated PTFE disks only, Ω
R_{st}	Standard electrolyte resistance, Ω
Z	Complex impedance, Ω
Z_{Im}	Imaginary part of complex impedance, Ω
Z_{Re}	Real part of complex impedance, Ω
ε	Total porosity, -
k_D	Conductivity of the electrolyte in the pores, $\Omega^{-1}cm^{-1}$
k_{st}	Standard electrolyte conductivity, $\Omega^{-1}cm^{-1}$
ρ_{el}	Ionic resistivity of the electrolyte, Ωcm
τ	Electric tortuosity, -
τ_{geo}	Geometric tortuosity, -
ω	Wettability factor, -

References

1. K. Zeng and D. Zhang, *Prog. Energy Combust.*, **36**, 307 (2010).
2. EU Commission Directive 1999/77/EC, http://www.eara.nl/1999-77.pdf.
3. M. García-Gabaldón, V. Pérez-Herranz, E. Sánchez, and S. Mestre, *J. Membr. Sci.*, **323**, 213 (2008).
4. Ph. Vermeiren, R. Leysen, H. Beckers, J. P. Moreels, and A. Claes, *J. Porous Mater.*, **15**(3), 259 (2008).
5. M. García-Gabaldón, V. Pérez-Herranz, E. Sánchez, and S. Mestre, *J. Membr. Sci.*, **280**, 536 (2006).
6. H. Wendt and G. Imarisio, *J. Appl. Electrochem.*, **18**, 1 (1988).
7. E. Guerrini and S. Trasatti, *Catalysis for Sustainable Energy Production*, Edited by P. Barbaro and C. Bianchini, Wiley-VCH, 2009.
8. P. Häussinger, R. Lohmüller, and A. M. Warson, *Ullmann's Encyclopedia of Industrial Chemistry*.
9. V. M. Rosa, M. B. F. Santos, and E. P. Da Silva, *Int. J. Hydrogen Energy*, **20**(9), 697 (1995).
10. IR. J. H. G. Van der Stegen, *J. Appl. Electrochem.*, **19**, 571 (1989).
11. D. Wiedenmann, L. Keller, L. Holzer, J. Stojadinović, B. Münch, and L. Suarez et al., 3D pore structure and ion conductivity of porous ceramic diaphragms, submitted to AIChE (2012).
12. D. Wiedenmann, Development and Characterisation of Porous Membranes for Electrolysis and Fuel Cell Applications, Fribourg 2011, Thesis No 1740.
13. A. Fievet, A. Szymczyk, B. Aoubiza, and J. Pagetti, *J. Membr. Sci.*, **168**, 87 (2000).
14. S. O. Engblom, J. C. Myland, K. B. Oldham, A. L. Taylor, and W. C. Topic, *J. Appl. Electrochem.*, **33**, 51 (2003).
15. G. E. Archie, *Trans. AIME*, **146**, 54 (1942).
16. D. S. McLachlan, M. Blaszkiewicz, and R. Newnham, *J. Am. Ceram. Soc.*, **73**, 2187 (1990).